

# Seasonal variability of surface and column carbon monoxide over megacity Paris, high altitude Jungfraujoch and Southern Hemispheric Wollongong stations

Yao Té<sup>1</sup>, Pascal Jeseck<sup>1</sup>, Bruno Franco<sup>2</sup>, Emmanuel Mahieu<sup>2</sup>, Nicholas Jones<sup>3</sup>, Clare Paton-Walsh<sup>3</sup>, David W. T. Griffith<sup>3</sup>, Rebecca R. Buchholz<sup>4</sup>, Juliette Hadji-Lazarou<sup>5</sup>, Daniel Hurtmans<sup>6</sup>, and Christof Janssen<sup>1</sup>

<sup>1</sup>LERMA-IPSL, Sorbonne Universités, UPMC Univ Paris 06, CNRS, Observatoire de Paris, PSL Research University, F-75005, Paris, France

<sup>2</sup>Institut d'Astrophysique et de Géophysique, Université de Liège, B-4000 Liège, Belgique

<sup>3</sup>Center for Atmospheric Chemistry, Faculty of Science, Medicine & Health, University of Wollongong NSW 2522 Australia

<sup>4</sup>Atmospheric Chemistry Observations & Modelling Laboratory, National Center for Atmospheric Research, Boulder, CO, USA

<sup>5</sup>Sorbonne Universités, UPMC Univ. Paris 06, Univ. Versailles St-Quentin, CNRS/INSU, UMR 8190, LATMOS-IPSL, Paris, France

<sup>6</sup>Spectroscopie de l'Atmosphère, Service de Chimie Quantique et Photophysique, Université Libre de Bruxelles, Brussels, Belgium

*Correspondence to:* Yao Té (yao-veng.te@upmc.fr)

**Abstract.** This paper studies the seasonal variation of surface and column CO at three different sites (Paris, Jungfraujoch and Wollongong), with an emphasis on establishing a link between the CO vertical distribution and the nature of CO emission sources. We find the first evidence of a time-lag between surface and free tropospheric CO seasonal variations in the Northern Hemisphere. The CO seasonal variability obtained from the total columns and from the free tropospheric partial columns shows a maximum around March-April and a minimum around September-October in the Northern Hemisphere (Paris and Jungfraujoch). In the Southern Hemisphere (Wollongong) this seasonal variability is shifted by about 6 months. Satellite observations by the IASI-MetOp and MOPITT instruments confirm this seasonality. Ground-based FTIR (Fourier Transform InfraRed) measurements provide useful complementary information due to good sensitivity in the boundary layer. In situ surface measurements of CO volume mixing ratios at Paris and Jungfraujoch reveal a time-lag of the near-surface seasonal variability of about 2 months with respect to the total column variability at the same sites. The chemical transport model GEOS-Chem is employed to interpret our observations. GEOS-Chem sensitivity runs identify the emission sources influencing the seasonal variation of CO. At both Paris and Jungfraujoch, the surface seasonality is mainly driven by anthropogenic emissions, while the total column seasonality is also controlled by air masses transported from distant sources.

At Wollongong, where the CO seasonality is mainly affected by biomass burning, no time shift is observed between surface measurements and total column data.

## 1 Introduction

20 Atmospheric carbon monoxide (CO) is an important trace gas. It has direct and indirect impact on air quality due to its toxicity and its effect on the atmospheric oxidizing capacity. The major sources of CO are fuel and energy-related industries, heating, motor vehicle transport, biomass burning, and the secondary oxidation of methane and of volatile organic compounds (VOCs such as isoprene and terpene, which are emitted by plants). Due to the fast reaction



CO is the major sink for the main atmospheric oxidation agent, the hydroxyl radical OH (Weinstock, 1969; Bakwin et al., 1994). A global increase of atmospheric CO thus leads to a decrease in global OH, which in turn augments the concentration of other, potentially harmful atmospheric trace gases (Logan et al., 1981; Thompson et al., 1990; Thompson, 1992) or potent greenhouse gases sensitive  
30 to oxidation such as methane, which contributes about one-third to the total sources of CO (Duncan et al., 2007; Holloway et al., 2000). The limited measurements before 1980 showed an increase of CO in the Northern Hemisphere (Khalil and Rasmussen, 1988; Zander et al., 1989), probably related to an increase of anthropogenic emissions (Novelli et al., 1998). From the end of 1980 until 1997, atmospheric CO decreased (Khalil and Rasmussen, 1994; Novelli et al., 1994). Since then, a few  
35 large episodic increases of CO, associated with unusually large forest fires, have been observed in the Northern Hemisphere (Novelli et al., 2003; Yurganov et al., 2004, 2005). Bekki et al. (1994) have observed a negative trend in CO, that was attributed to the Mount Pinatubo eruption in June 1991. In the Southern Hemisphere no significant trends were observed (Brunke et al., 1990; Novelli et al., 2003). Global observations of CO began with the start of the flask sampling program of the NOAA<sup>1</sup>  
40 Earth System Research Laboratory, Global Monitoring Division (Novelli et al., 1994, 1998, 2003). In parallel, CO total column observations were performed at several locations (Mahieu et al., 1997; Zhao et al., 1997; Rinsland et al., 1998, 1999, 2000).

This paper characterizes the CO seasonal variability at three ground-based FTIR sites: Paris megacity, high-altitude Jungfraujoch and Southern Hemisphere Wollongong. These sites have been  
45 selected for their representativeness of different environments (remote vs. moderate and high pollution sites, Northern vs. Southern Hemisphere) and meteorological conditions:

- Megacity of Paris (France): A high-resolution Fourier transform spectrometer from Bruker IFS 125HR (FTS-Paris) has been installed in 2006 on the campus of “Université Pierre et

---

<sup>1</sup>National Oceanic and Atmospheric Administration

Marie Curie” in the centre of the French capital Paris (48°50'47"N, 2°21'21"E, 60 m asl).

50 Since then, the instrument has been continuously operated by LERMA<sup>2</sup>.

– Jungfrauoch (Switzerland): The International Scientific Station of the Jungfrauoch (ISSJ) is located in the Swiss Alps (46°33'N, 7°58'48"E, 3580 m asl). Two FTIR instruments have been used at that site, a homemade FTIR from 1984 to 2008 and a commercial Bruker IFS 120 HR from the early 1990 to present. University of Liège (Belgium) is responsible for the operation  
55 of the infrared instruments at Jungfrauoch.

– Wollongong (Australia): The station is located in the Southern Hemisphere at Wollongong University (34°24'22"S, 150°52'44"E, 30 m asl). The instrument, which is also a commercial high-resolution Fourier transform spectrometer (Bruker IFS 125HR), is operated by the University of Wollongong and provides data since 1996.

60 All three ground-based FTIR spectrometers are part of NDACC (Network for the Detection of Atmospheric Composition Change) and/or TCCON (Total Carbon Column Observing Network) networks and have monitored the concentration of CO for several years. Paris is the first ground-based FTIR station located in a European megacity, which provides rare hot spot measurements of atmospheric species related to anthropogenic activities. The remote high-altitude Jungfrauoch station provides  
65 one of the longest observational time series for a variety of atmospheric gases. Wollongong is a station exposed to moderate levels of pollution and is located on the East coast of Australia, about 80 km from the south of Sydney. Here, we analyse NDACC data for the seasonal variations of CO and compare the results from the different sites. The ground-based remote sensing measurements are compared with results from the satellite instruments IASI-MetOp (Infrared Atmospheric Sounding  
70 Interferometer (Tournier et al., 2002)) and MOPITT (Measurements Of Pollution In The Troposphere (Drummond and Mand, 1996)). With respect to satellite measurements, ground-based FTIR instruments are more sensitive to the boundary layer and can therefore provide complementary information which we compare with in situ measurements at the surface. Due to specific conditions at the ground, the surface and the total column seasonalities might differ from each other. Using  
75 GEOS-Chem modeling (Goddard Earth Observing System - chemical transport model (CTM), Bey et al. (2001)) simulations, we investigate the impact of local sources on the lower partial column and its variability as compared to the total column.

The paper is structured as follows. In section 2, the remote sensing instruments and measurements are described. Section 3 presents the in situ analyser measurements and the GEOS-Chem model  
80 simulation data. Section 4 shows the CO total column variability obtained from both the remote sensing data and the surface in situ measurements. Both results are compared to the GEOS-Chem model simulations, which is also used to identify emission sources at each site.

---

<sup>2</sup>Laboratoire d'études du Rayonnement et de la Matière en Astrophysique et Atmosphères

## 2 Remote sensing instruments and measurements

### 2.1 Instrumentation and measurements at Paris, France

85 The FTS-Paris is a Michelson interferometer from Bruker Optics. Table 1 lists technical details for the ground-based FTIR instruments as well as the configuration used for the measurements. Solar absorption spectra are acquired by coupling the FTS to a sun-tracker installed on the roof terrace. The solar disk is tracked with an accuracy of less than 1 arcmin. Appropriate band pass filters allows the optimisation of the signal-to-noise ratio when focussing on specific target gases.

90 The Paris instrument is part of TCCON (TCCON-Paris station). For this CO study, the FTS-Paris uses optical elements corresponding to a typical NDACC configuration. More instrumental details and different measurement configurations are given elsewhere (Té et al., 2010, 2012).

Only clear sky spectra were analysed. Available solar spectra cover the time period from May 2009 to the end of 2013, with only very few spectra (about 400 spectra during 19 measurement

95 days) for the period between 2009 and 2010. Between 2011 and 2013, spectra acquisition was more frequent and more than 4500 spectra from 117 measurement days were recorded and analysed. The absorption lines of each atmospheric species observed in the solar spectra are used to retrieve its abundance in the atmosphere by appropriate radiative transfer and inversion algorithms (Pougatchev and Rinsland, 1995; Zhao et al., 1997; Hase et al., 2006). We have used the PROFFIT algorithm

100 developed by F. Hase to analyse the Paris data using the HITRAN 2008 spectral database (Rothman et al., 2009). PROFFIT is a code especially adapted for the analysis of solar absorption spectra from the ground and it has been widely applied and tested (Hase et al., 2004; Duchatelet et al., 2010; Schneider et al., 2010; Té et al., 2012; Viatte et al., 2011). For the retrieval of CO, we have selected two micro-windows. The  $2110.4 - 2110.5 \text{ cm}^{-1}$  micro-window is centred around the weak

105  $R(3)$  line of  $^{13}\text{CO}$ , which is more sensitive to CO at higher altitudes and the  $2111.1 - 2112.1 \text{ cm}^{-1}$  micro-window around the strongly saturated  $P(8)$  line of  $^{12}\text{CO}$ . The left and right wings of the  $P(8)$  line are particularly sensitive to CO in the Planetary Boundary Layer (PBL). The retrieval uses a grid with 49 altitude levels and, on average, there are about 2.7 degrees of freedom for signal (DOFS). The uncertainties in the CO column density and the profile stem from a variety of sources.

110 These sources have been investigated in detail by Té et al. (2012), following the procedure outlined by Rinsland et al. (2000). According to this evaluation, the random uncertainty is around 2.5%. Concerning the systematic uncertainties of about 3 to 6.8% (Té et al., 2012), the largest source is linked to the quality of available spectroscopic parameters (line intensity and air-broadened half-width uncertainties in Rothman et al. (2009)), which is similar for the three sites.

### 115 2.2 Instrumentation and measurements at Jungfraujoch, Switzerland

The Jungfraujoch station in Switzerland is part of NDACC and the instrumental setup is similar to the one in Paris, cf. Table 1. A thorough description of the instrumentation is given by Zander

et al. (2008). Infrared solar spectra are recorded under clear-sky conditions and, due to the high altitude, the interference by water vapour is very low. The integration time is either 135, 404 or 1035 s, corresponding to 3 or 9 scans of 45 s, or 15 scans of 69 s. High resolution observations are only recorded under slowly varying geometry, i.e. for zenith angles lower than  $\sim 70^\circ$ .

The Jungfraujoch data set corresponds to an update of the CO time series described by Dils et al. (2011). It covers the January 2009 to December 2013 time period and includes 1733 individual spectra recorded on 539 different days. Mean signal-to-noise ratio (S/N) is 2930, with the 2<sup>nd</sup> percentile still being above 1000. The SFIT-2 (v3.91) algorithm (Rinsland et al., 1998) based on the semi-empirical implementation of the Optimal Estimation Method (OEM) of Rodgers (1990) is used, allowing retrieval of information on the vertical profile of most FTIR target gases. The standard NDACC approach for the CO retrieval is adopted, to simultaneously fit three micro-windows spanning the 2057.7 – 2058.0, 2069.56 – 2069.76 and 2157.3 – 2159.15  $\text{cm}^{-1}$  intervals. The line parameters correspond to the standard release of HITRAN 2004 (Rothman et al., 2005), including the August 2006 updates (e.g. Esposito et al., 2007). The a priori mixing ratio profiles for all interfering molecules (main telluric absorptions by  $\text{N}_2\text{O}$ ,  $\text{O}_3$ ,  $\text{H}_2\text{O}$  and  $\text{CO}_2$ ) correspond to a mean of the 1975-2020 version 4 WACCM model (the Whole Atmosphere Community Climate Model; <https://www2.cesm.ucar.edu/working-groups/wawg>) simulation performed for Jungfraujoch. The CO a priori vertical distribution combines version 4 WACCM results above 15.5 km, ACE-FTS occultation measurements between 6.5 and 15.5 km (version 2.2, Clerbaux et al., 2008) and extrapolation of ACE-FTS data down to the station altitude, ending at 137 ppbv in the first retrieval layer (3.58 – 4.23 km). Additional retrieval settings include a S/N ratio of 150 for inversion, the a priori covariance matrix, with diagonal elements close to 30%/km in the troposphere and extra-diagonal elements computed assuming a Gaussian inter-layer correlation half-width length of 4 km. Objective evaluation of the resulting typical information content indicates that 2 independent pieces of information are available (DOFS of 2.2 on average). Typical random uncertainties have been evaluated at 2 – 3% for the total columns and 5% for the 3.58 – 7.18 km partial columns.

### 2.3 Instrumentation and measurements at Wollongong, Australia

The Wollongong instrument is part of both NDACC and TCCON. The instrument setup is similar to the Paris and Jungfraujoch spectrometers (see Table 1). Using the NDACC configuration, CO total and partial column data are produced using 3 micro-windows in the 4.6  $\mu\text{m}$  band of CO (Zeng et al., 2015).

The analysis of the Wollongong NDACC data is very similar to the method described in section 2.2 for the Jungfraujoch data. The algorithm used was SFIT4 v9.4.4 (<https://wiki.ucar.edu/display/sfit4/Infrared+Working+Group+Retrieval+Code,+SFIT>), an updated version of SFIT2 used in the Jungfraujoch analysis. SFIT4 has inherited the same forward model and inverse method but with a number of enhancements (not required in the CO analysis), and gives the same results in the CO

retrieval. For the Wollongong data, HITRAN 2008 was adopted (Rothman et al, 2009), the mean of  
155 the 1980-2020 WACCM version 4 run used as the a priori CO profile (and a 4 km Gaussian interlayer  
correlation), with the a priori covariance matrix set to 1 standard deviation of the WACCM profiles.  
A measurement signal-to-noise ratio of 200 was assumed. This gives a mean DOFS of 2.7. The  
version 4 WACCM profiles were also used for the a priori profiles of all actively fitted interfering  
gases (O<sub>3</sub>, H<sub>2</sub>O, N<sub>2</sub>O, CO<sub>2</sub>, etc.). The error analysis used a NDACC community Python tool to  
160 estimate errors assuming a solar zenith angle of 50.2°, representing the mean zenith angle for all  
Wollongong spectra. The resulting CO total column random errors were calculated to be 2.2%.

## 2.4 Satellite instruments and measurements

The IASI Michelson interferometer (Infrared Atmospheric Sounding Interferometer, Tournier et al.  
(2002); Blumstein et al. (2004)) is flying on-board the Meteorological operation (MetOp) polar Orbit  
165 platform. The first platform (MetOp-A) was launched on October 19, 2006 and operational data  
have been provided since October 2007. IASI operates at an altitude of around 817 km on a sun-  
synchronous orbit with a 98.7° inclination to the equator. It overpasses each region twice a day.  
The MetOp platform has a swath of 30 views of 50 km by 50 km comprising four off-axis pixels of  
12 km diameter footprint each at nadir. A second platform (MetOp-B) was launched in September  
170 2012 and the launch of the third and last platform (MetOp-C) is scheduled for October 2018. IASI  
observations provide an important contribution to the monitoring of atmospheric composition over  
time (Clerbaux et al., 2009).

The IASI-MetOp is a Fourier transform spectrometer with a medium spectral resolution of 0.5 cm<sup>-1</sup>  
and a radiometric noise of about 0.2 K at 280 K using nadir viewing and working in the thermal in-  
175 frared (TIR) range extending from 645 to 2760 cm<sup>-1</sup> with no gaps. The CO products (L2) are down-  
loaded from the ETHER database, cf. <http://www.pole-ether.fr>, for the period from January 1, 2009  
to December 31, 2013. The total column data were generated from the IASI radiance spectra in the  
4.7 μm spectral range and from meteorological data (surface and vertical profile of temperature, hu-  
midity vertical profile and cloud cover) (August et al., 2012), using the Fast Optimal Retrievals on  
180 Layers for IASI (FORLI) code (Hurtmans et al., 2006). The CO total columns were compared to  
other CO satellite data (George et al., 2009), from which a DOFS value of about 2 was provided  
and a relative uncertainty between 4% and 10% could be estimated. The total columns are calculated  
from the ground altitude to 60 km height. For this paper, we also provide additional vertical volume  
mixing ratio (VMR) profiles and partial columns in the PBL and in the troposphere layers around  
185 Île-de-France; as well as the partial columns above 4 km height around the Jungfraujoeh site.

The MOPITT instrument (Drummond and Mand, 1996; Deeter et al., 2004) is on-board NASA's  
Terra spacecraft in a sun-synchronous polar orbit at an altitude of 705 km. The satellite was launched  
on December 18, 1999. MOPITT has been operational since March 2000. The instrument uses the

190 technique of gas-filter correlation radiometry based on the IR absorption bands of CO to retrieve the vertical profiles of CO. The horizontal footprint of each MOPITT retrieval is 22 km by 22 km.

The MOPITT data were downloaded from the NASA website, cf. <https://eosweb.larc.nasa.gov/datapool>. We are using version 6 retrievals of CO vertical profiles and total columns, for the period from the beginning of 2009 to the end of 2013. The MOPITT retrieval history can be found at the link <https://www2.acd.ucar.edu/mopitt/products>. Since version 5 of the MOPITT retrieval algorithm, TIR (4.7  $\mu\text{m}$ ) radiances are combined with the near IR (2.3  $\mu\text{m}$ ) daily radiances to improve the sensitivity to lower tropospheric CO over land. The DOFS value is about 2 (Worden et al., 2010). The retrieved vertical VMR profile is reported on 10 pressure levels (at the surface and every hundred hPa between 900 and 100 hPa). The retrieved CO total columns are obtained by integrating the retrieved VMR profile. In this paper, we are using the level 2 TIR/NIR products.

200 The following precautions have been taken in order to improve comparability between satellite and ground based measurements:

- Only clear sky data from ground-based FTIR and satellites has been used.
- The CO abundance is retrieved from the same spectral domain (4.7  $\mu\text{m}$  for both the ground-based FTIR and the satellite instruments), allowing to minimize possible biases related to spectroscopic parameters and interfering atmospheric constituents (gaseous species, aerosols).
- Satellite data were selected within a 30 km  $\times$  30 km square centered at the site location: corresponding to a range of  $\pm 0.15^\circ$  for the latitude and  $\pm 0.23^\circ$  for the longitude.

### 3 In situ analyser measurements and GEOS-Chem model simulation data

#### 3.1 Surface in situ measurements at Paris

210 Continuous in situ measurements of the CO surface concentration are performed using a commercial analyser (CO11M, Environnement SA). The operating principle of the CO analyser is based on the CO infrared absorption at 4.67  $\mu\text{m}$ , which is the same spectral band covered by the FTS-Paris. Ambient atmospheric air is drawn from the building rooftop into the analyser via PTFE tubing using a diaphragm pump, which is limited to a gas flow of 80 litres per hour. The pumped air is analysed in a 20 cm length multi-path absorption cell with an absorption path length of 5.6 m, using a global IR source and a photoconductive PbSe detector. The CO analyser has a sensitive range between 0.1 and 200 ppmv, with an uncertainty of 50 ppbv for each individual measurement. Recorded values are time averages over 15 minutes. For the present paper, daily in situ surface CO measurements are available for the whole period between beginning of 2009 and end of 2013.

## 220 **3.2 Surface in situ measurements in Switzerland**

Swiss in situ surface data are from the Swiss National Air Pollution Monitoring Network (NABEL), which is a network of 16 observation sites distributed throughout Switzerland in order to measure and record long-term measurement series of air pollutants. The NABEL monitoring network is operated by EMPA. The monitoring stations are representative of different pollution levels. The monthly  
225 averaged data were obtained from the annual reports published by the Swiss OFEV (Office fédéral de l'Environnement, <http://www.bafu.admin.ch/publikationen/00016>). In this paper, we have focussed on the urban sites Bern, Lausanne, Lugano and Zürich, as well as the remote mountain station of Jungfrauoch.

## **3.3 Surface in situ measurements at Wollongong**

230 Surface CO at Wollongong is measured using two high-precision in situ FTIR trace gas analysers (Griffith et al., 2012). The analysers use an IR source, modulated through a Michelson interferometer with a CaF<sub>2</sub> beamsplitter. The modulated IR beam is passed through a dried atmospheric sample within a White cell in a 24 m folded-path and subsequently detected by thermoelectrically cooled MCT (Mercury Cadmium Telluride) detector. Ambient air is measured daily over 23.5 hours, with  
235 30 minutes reserved for calibration using constant composition air. Ambient air is flushed through an inlet line at 5 L/min and sample air is continuously drawn from this line through the instrument at 1 L/min. The Spectronus<sup>TM</sup> software (Ecotech P/L, Knoxfield, VIC, Australia) is used to automate internal valve control and stabilise parameters, such as flow, pressure and temperature. Recorded spectra are averaged over 3 minutes. Non-linear least-squares fitting of CO occurs in two broad  
240 spectral regions (from 4.33 to 4.65  $\mu\text{m}$  and from 4.46 to 4.76  $\mu\text{m}$ ), using the program MALT (Multiple Atmospheric Layer Transmission, Griffith (1996)). Data are reported as dry-air mole fraction, with a total relative measurement uncertainty below 1%. Wollongong CO measurements were first analysed by Buchholz et al. (2016) and are publicly available as 10 minute averages via PANGAEA (doi:10.1594/PANGAEA.848263). For this paper, in situ data is monthly averaged and selected to  
245 cover the period from June 2012 to May 2013.

## **3.4 Data from the GEOS-Chem model**

The global 3-D chemical transport model GEOS-Chem (version 9-02: <http://acmg.seas.harvard.edu/geos/doc/archive/man.v9-02>) can be used to simulate global trace gas (more than 100 tracers) and aerosol distributions. The model is driven by the Goddard Earth Observing System v5 (GEOS-5)  
250 assimilated meteorological fields from the NASA Global Modeling Assimilation Office (GMAO), which are at a native horizontal resolution of  $0.5^\circ \times 0.667^\circ$ . The GEOS-5 data describe the atmosphere from the surface up to 0.01 hPa with 72 hybrid pressure- $\sigma$  levels, at a 6 h temporal frequency (3 h for surface properties and mixing depths). In this study, we use the degraded GEOS-5 meteo-



255 rological fields as model input to a  $2^\circ \times 2.5^\circ$  horizontal resolution and 47 vertical levels, lumping  
together levels above  $\sim 80$  hPa. We apply here the standard full chemistry GEOS-Chem simulation,  
including detailed  $O_3 - NO_x -$  Volatile Organic Compound (VOC) – aerosol coupled chemistry (Bey  
et al. (2001); Park et al. (2004); with updates by Mao et al. (2010)).

Tropospheric CO is sourced from anthropogenic, biomass burning and biofuel burning emissions,  
as well as from the degradation of many VOCs. The emission inventory of the emissions database for  
260 Global Atmospheric Research (EDGAR; <http://edgar.jrc.ec.europa.eu>) v3.2 (Olivier and Berdowski,  
2001) is the global reference for anthropogenic emissions of CO,  $NO_x$ ,  $SO_x$ , and  $NH_3$ . For global  
anthropogenic sources of Non-Methane VOCs (NMVOCs), GEOS-Chem uses the REanalysis of the  
TROspheric chemical composition (RETRO; [http://gcmd.gsfc.nasa.gov/records/GCMD\\_GEIA\\_](http://gcmd.gsfc.nasa.gov/records/GCMD_GEIA_RETRO)  
RETRO) emission inventory (Schultz et al., 2007) for the base year 2000. However, these global  
265 inventories may be overwritten by regional emission inventories such as over Europe, where the  
anthropogenic emissions of CO,  $NO_x$ ,  $SO_x$ ,  $NH_3$ , propene, acetaldehyde, methyl ethyl ketone and  
higher C3 alkanes are provided by the European Monitoring and Evaluation Programme (EMEP;  
<http://www.ceip.at>) regional inventory for the year 2010 (Benedictow et al., 2010). All these global  
and regional inventories are scaled to the years of interest according to the method described by van  
270 Donkelaar et al. (2008). Anthropogenic sources of ethane and propane are derived from an offline  
simulation (Xiao et al., 2008). The global biomass burning emissions are provided by the Global Fire  
Emissions Database (GFED) v3 (van der Werf et al., 2010) and the global biogenic emissions are  
obtained with the Model of Emissions of Gases and Aerosols from Nature (MEGAN) v2.1 (Guenther  
et al., 2006)). Methane concentrations in GEOS-Chem are based on measurements from the NOAA  
275 Global Monitoring Division flask measurements.

The GEOS-Chem data set employed in the present work covers the period from January 2009  
to May 2013 and is derived from a July 2005 to May 2013 simulation, for which the GEOS-5  
meteorological fields are available. A 1-year run preceding this simulation was used for chemical  
initialization of the model. The model outputs consist of CO VMR profiles simulated at the closest  
280 pixel to each station and saved at a 3 h time step. The vertical resolution and the sensitivity of the  
FTIR retrievals have been taken into account for the comparisons involving GEOS-Chem results:  
the individual VMR profiles produced by the model have been first regridded onto the vertical layer-  
scheme adopted at each station, then daily averaged and finally smoothed by convolution with the  
FTIR averaging kernels (AVKs) according to the formalism of Rodgers and Connor (2003). The  
285 regridding method used here is a mass conservative interpolation that preserves the CO total mass  
simulated above the altitude of the station (the CO mass below is ignored). The AVKs employed  
for smoothing are seasonal averages (over March – May, June – August, September – November  
and December – February, respectively) derived from the individual retrievals of the 2009 – 2013  
FTIR data sets. The smoothing did not change the comparison results between the model and our  
290 observations (difference smaller than 1%).

## 4 Seasonal variability

### 4.1 Remote sensing observations

Figure 1 shows the CO total columns of the three ground-based FTIR sites from 2009 to the end of 2013. The data from Paris are less numerous than from the other two sites, because measurements are not fully automated and spectral acquisitions are only launched when clear sky is expected for more than half of the daytime. Moreover, from 2009 to 2010, Paris CO spectra were recorded only during intensive measurement campaigns, and not on a regular basis. As expected, the CO abundance is higher in the Northern Hemisphere. The CO column mean value is about  $2.1 \times 10^{18}$  molecules/cm<sup>2</sup> at Paris which is almost twice as high as the value at Wollongong ( $1.3 \times 10^{18}$  molecules/cm<sup>2</sup>). The CO column mean value of  $1.1 \times 10^{18}$  molecules/cm<sup>2</sup> at Jungfraujoch is quite low and is attributed to the site's height.

All three sites clearly display a seasonal variability of CO. We have used a sine function to characterize seasonality (Eq. (1)). This is in agreement with previous studies conducted by Rinsland et al. (2000, 2001, 2007) and Zhao et al. (2002), but in comparison to Rinsland et al., we have removed the linear term, because our data sets do not show any significant trend:

$$y = y_0 + A \sin\left(\pi \frac{t - t_c}{w}\right). \quad (1)$$

Where  $y$  represents the abundance of CO (in total or partial columns or volume mixing ratio);  $y_0$  is the mean value (offset);  $A$  and  $w$  respectively are the amplitude and the half-period of the seasonal cycle;  $t$  and  $t_c$  the date and the phase shift. Table 2 summarizes the fit results for  $w$  and  $A$  obtained at the three sites.

For the Northern Hemisphere (Paris and Jungfraujoch), the maximum is observed around March-April and the minimum around September-October. The average amplitude of the seasonal variability is about  $(13 \pm 3)\%$  of the column average and the average half-cycle is about  $188 \pm 4$  days for both Northern hemispheric sites. For Paris, the value  $w = 191 \pm 3$  days is slightly, but not significantly, higher than at Jungfraujoch probably due to the lack of data before 2011. This seasonal variability is also observed by Rinsland et al. (2007) at Kitt Peak, which is the US National Solar Observatory at 2.09 km altitude located in the Northern Hemisphere, by Barret et al. (2003) at the Jungfraujoch, and by Zhao et al. (2002) for Northern Japan. Our observations also agree with a recent 11 years climatology on purely tropospheric CO columns at Northern hemispheric sites (Zbinden et al., 2013), where observed maxima fall within the period from February to April. In the Southern Hemisphere, we observe an expected shift of 6 months as compared to the Northern Hemisphere, with a maximum in October and a minimum in April. The average half-period is about  $178 \pm 1$  days. We also note that the relative amplitude of the seasonal variation is slightly higher at Wollongong (17%) than at Paris, but it remains close within error bars. Interestingly, the relative amplitude is lowest at Jungfraujoch, where the impact of the local surface emissions is small.

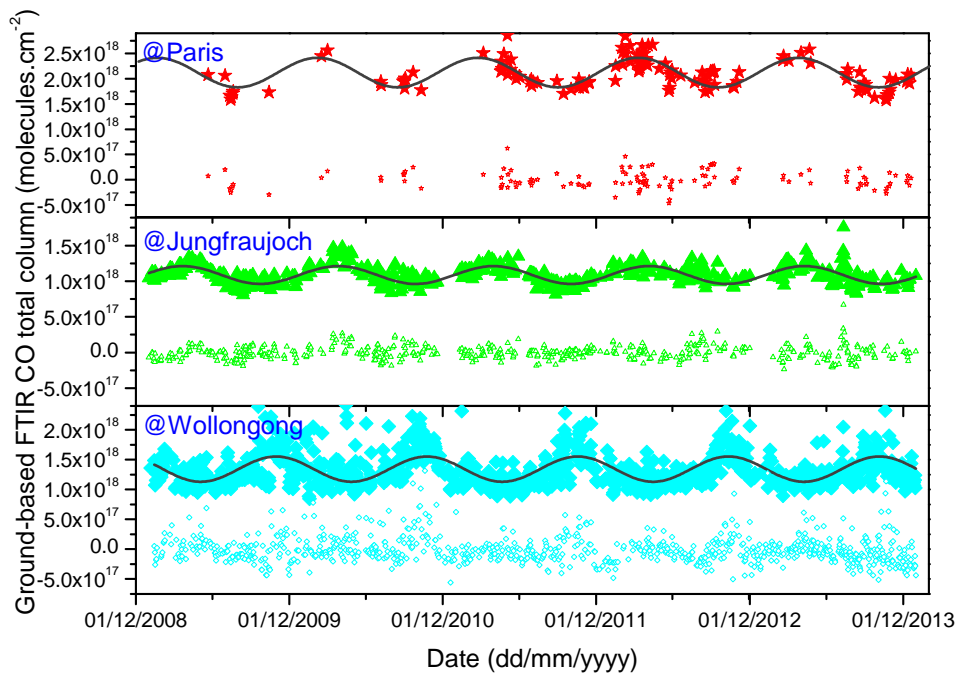


**Figure 1.** CO total columns retrieved by ground-based FTIR instruments at Paris (top), Jungfraujoch (middle) and Wollongong (bottom). Dark gray lines present CO seasonal variability at each station fitted with sine functions. Open symbols represent the residuals from the sine fit.

The seasonal variability of CO is also observed by the IASI-MetOp and MOPITT instruments, cf. Fig. 2 and Table 2. One of the advantages of the satellite measurements is their spatial coverage. In general, the period and the amplitude of the seasonal variability obtained from the satellite data agree with the corresponding values from the ground-based FTIR measurements. For the Jungfraujoch station, the satellite data need to be recalculated in order to correspond to the column between the ground altitude and the top of the atmosphere (Barret et al., 2003), because the large satellite footprint not only includes the site, but also neighboring areas of lower altitude. Concerning the IASI-MetOp data, the contributions from levels below the Jungfraujoch altitude have been subtracted from the total columns. For the MOPITT data, we extracted the retrieved CO profile for Jungfraujoch and interpolated the lower pressure levels onto thinner vertical grid in order to calculate the column between the given ground altitude and the top of the atmosphere. MOPITT measurements are performed for specific ground altitudes which, however, are not made available. We have assumed a ground altitude of about 1100 m which is the mean altitude for the Bern canton,<sup>3</sup> to which the Jungfraujoch belongs. Partial columns above 1100 m were then calculated using the interpolated CO vertical profiles and daily NCEP meteorological pressure and temperature profiles. Data from

<sup>3</sup><https://lta.cr.usgs.gov/GTOPO30> (Global 30 Arc-Second Elevation)

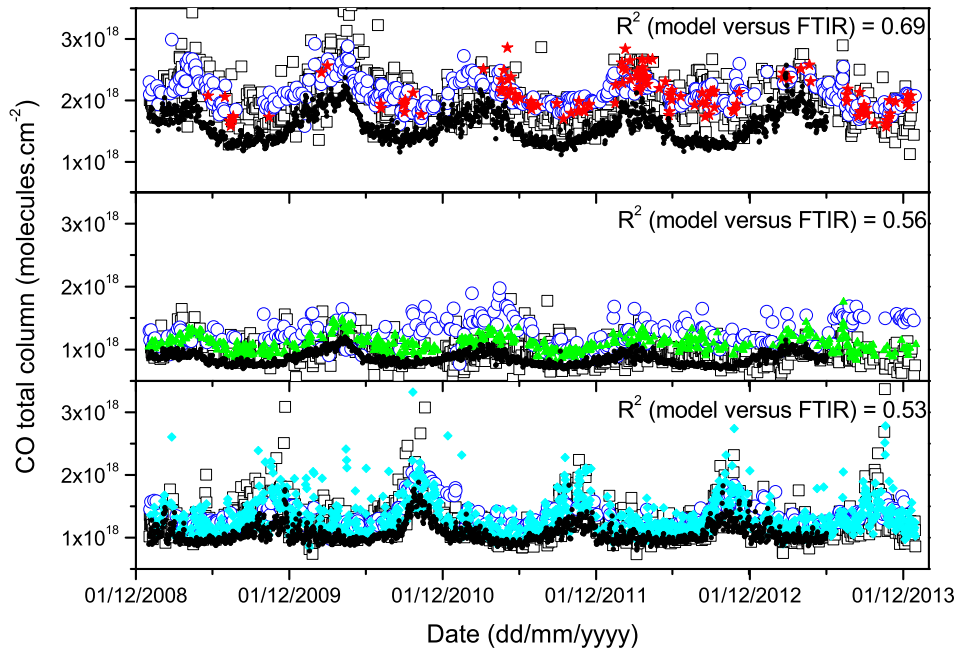


**Figure 2.** Time series of CO columns from satellite instruments and ground-based FTIR are given for Paris, Jungfraujoch and Wollongong (from top to bottom). IASI-MetOp and MOPITT columns are displayed as black open squares and blue open circles. Ground-based FTIR CO total columns are shown by red stars, green triangles and cyan diamonds for Paris, Jungfraujoch and Wollongong, respectively. GEOS-Chem CO total columns are indicated by black full circles.

the ground-based FTIR instruments and the satellites are in good agreement. This is demonstrated in Fig. 3, where the satellite data are plotted against the ground-based measurements. The good agreement is indicated by robust fits yielding slopes of 0.98 for Paris, 0.91 for Jungfraujoch and 0.99 for Wollongong. The robust fit regression is based on a process called iteratively reweighted least squares (Street et al., 1988) and is less sensitive than ordinary least squares to large changes in small parts of the data.

GEOS-Chem model outputs are presented in Fig. 2 for the entire period from the beginning of 2009 until June 2013. The model is in good agreement with ground-based observations ( $R^2$  between 0.53 and 0.69), even if the observed total atmospheric CO abundance is underestimated at all three sites: the relative deviations are commensurate:  $-24\%$  for Paris,  $-21\%$  for Jungfraujoch, and  $-20\%$  for Wollongong. In Duncan et al. (2007), the averaged bias between observations and GEOS-Chem model simulations is less than  $\pm 10\%$ , but for some sites (Seychelles or Tae-Ahn), the bias can exceed  $\pm 20\%$ . Zeng et al. (2015) have observed large underestimations from models when compared to the ground-based FTIR stations in the Southern Hemisphere ranging from  $-19.2\%$  to  $-27.5\%$

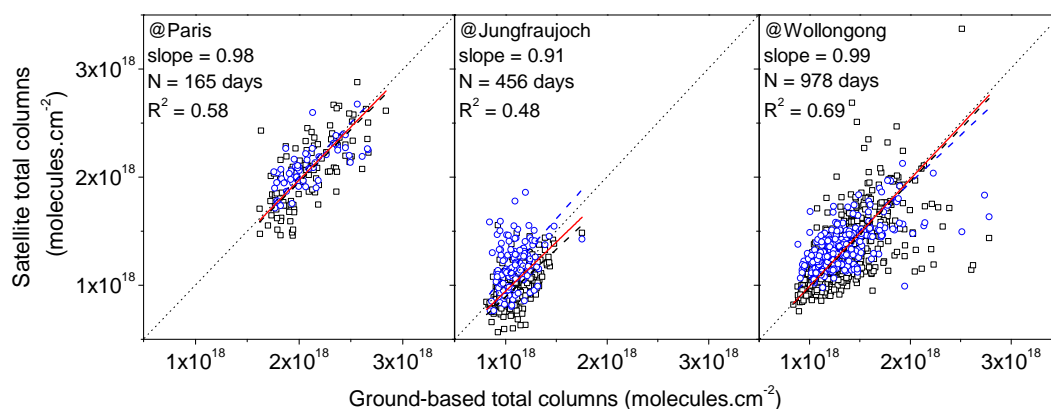


**Figure 3.** Correlation between satellites (IASI and MOPITT) and ground-based FTIR total columns at the three different sites, IASI data are in black squares and MOPITT data in blue circles. The dark dotted line and the blue dotted line are the robust regression fit results for respectively IASI-MetOp and MOPITT. Slope values are obtained using both data sets (red line).

355 and concluded differences depend on the emission inventories implemented in the models for the Wollongong site (episodic events are unaccounted for in the emission inventories). The present deviations are also consistent with previous inverse modeling studies (Kopacz et al., 2010; Hooghiemstra et al., 2012) and could originate from an underestimation of the emissions of CO and of its VOC precursors in the inventories currently implemented in GEOS-Chem. Nonetheless, exploring this  
 360 discrepancy was beyond the scope of this paper that aims at studying the seasonal variability of CO rather than reproducing observed concentrations. It has thus to be underlined that the model shows the same seasonal variability as the measurements: GEOS-Chem simulations reproduce the Northern Hemisphere maximum in March-April and the minimum in September-October and the model is therefore appropriate for diagnosing the seasonal variability. Both, the period and the relative amplitude of the variability are comparable to the measurement results, cf. Table 2. The lower  
 365  $R^2$  between GEOS-Chem and ground-based FTIR for Jungfraujoch and Wollongong as compared to Paris, are probably due to the more complex orography at these two sites: Jungfraujoch is located in the highest Swiss Alps and the surroundings show very large differences in altitude; Wollongong is sandwiched between the ocean (Tasman sea) and a mountainous region (Blue mountains) with a  
 370 typical altitude of a few hundred meters.

## 4.2 In situ measurements of surface CO

Daily averages of the surface CO concentration during the 2009 – 2013 period at Paris are plotted in the bottom panel of Fig. 4. Since only very few FTS-Paris data are available for the winter months January and December, the corresponding monthly means have not been presented in Fig. 4.

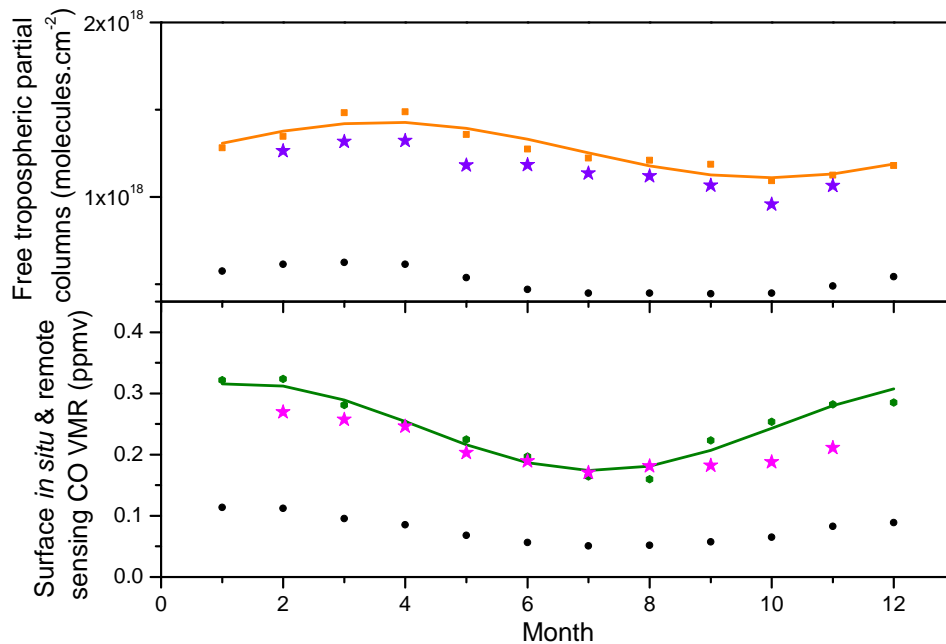


**Figure 4.** Free tropospheric (top) and surface (bottom) CO at Paris as monthly averages over 5 years. CO VMR in the PBL comes from the in situ CO analyser (dark green hexagons) and from the FTS-Paris (magenta stars), as well as from the GEOS-Chem model (black circles). Free tropospheric CO columns were calculated between 2 and 12 km and monthly averaged over the period from 2009 to 2013. Shown are data from IASI-MetOp (orange squares), FTS-Paris (purple stars) and from GEOS-Chem modeling (black circles). A sine function fit is applied to the IASI-MetOp (orange line) and in situ CO data (dark green line).

375 The figure shows a clear seasonal variability with a maximum around January-February and a  
 380 minimum around July-August. The amplitude of the seasonal variation is about 30%, which is larger  
 than the total column variability. This shows the stronger and more direct influence of local CO  
 emissions due to anthropogenic activities, which are expected to be particularly high in a megacity.  
 As mentioned in Sect. 2.1, the retrieval grid (49 levels) provides a much thinner atmospheric layering  
 than the effective vertical resolution indicated by the averaging kernels (Rodgers, 1990). The CO  
 averaging kernels for each altitude of the a priori profile indicate a good sensitivity of the FTS-  
 Paris instrument to the PBL. Effectively, the left panel of the Fig. 5 shows that the retrieval of CO  
 essentially provides two independent measurements of tropospheric CO: the first supplies maximal  
 information in the altitude range between 0 and 1000 m and thus well represents the PBL. The  
 385 comparability between FTIR retrievals and surface in situ observations is thus assured. The second  
 one is representative of the upper troposphere, with a maximum around 8-9 km. The FTS-Paris data  
 in the bottom panel of Fig. 4 represent the averaged CO VMR obtained for the altitude range between

the ground (60 m asl) and the 1000 m level. These remote sensing measurements are consistent with the in situ data, even if they are much less affected by local pollution peaks. By comparing Figs. 1 and 390 4, we notice that the seasonal variability of the total column is shifted by about 2 months as compared to the variability at the surface. The free tropospheric columns of CO have been calculated as partial columns between 2 and about 12 km over Paris for both, IASI-MetOp and FTS-Paris. The right panel of the Fig. 5 shows the July 2010 monthly averaged AVKs of IASI-MetOp. These AVKs show a relatively low surface sensitivity which is more emphasised during winter (we have also checked 395 the January 2010 monthly averaged AVKs not shown here). We thus only exploit the partial columns corresponding to the free troposphere. The seasonal variability in the free troposphere obtained by the three different kinds of data is also shifted by two months as compared to the surface seasonal variation. In addition to local surface sources, column abundances are influenced by the transport of downwind emission sources. The surface seasonal variability is directly influenced by the local 400 emission due to human activities: fossil fuel combustion, domestic heating, and industrial activities. In contrast, the total column seasonal variability is additionally influenced by emissions from distant sources that get transported into the upper levels of the atmosphere. The surface CO maximum in January-February corresponds to the winter season, where domestic heating is strong and where the PBL height is reduced. Additionally, oxidation by OH is lowest due to weak actinic flux. The 405 minimum in July-August, where the PBL height is highest, not only corresponds to an increased oxidization of CO by OH, whose abundance is influenced by solar ultraviolet radiation (Bousquet et al., 2005; Rohrer and Berresheim, 2006; Duncan et al., 2007), but also to the summer vacation season during which the inhabitants of Paris usually leave the city (by more than 50%, <http://www.insee.fr>), leading to a drastic decrease of vehicle traffic. In order to check the consistency of the 410 GEOS-Chem model, we have plotted the GEOS-Chem surface VMR in the bottom panel of the Fig. 4. The model confirms the time shift between surface and total column seasonal variability, with a surface maximum at the end of January-February and a minimum at the end of July-August. We once again notice an underestimation of the surface CO VMR by the GEOS-Chem model. The discrepancy of about  $-37\%$  is larger than the difference of  $-24\%$  between GEOS-Chem and ground- 415 based total columns, and can probably be attributed to strong local emissions, which are not in the current emission inventories implemented in GEOS-Chem.

There is also a temporal shift in seasonal variations between the surface and the high altitudes in Switzerland, as indicated by the difference between urban and mountain sites. This is shown in Figure 6 that compares the four urban NABEL sites with an average altitude of 438.25 m asl to the 420 in situ surface CO obtained on top of Jungfrauoch at the altitude of 3578 m asl. The low-altitude sites show a similar seasonal variability to the surface CO at Paris, with a maximum around January and a minimum around July. Zellweger et al. (2009) point out that the in situ observations at Swiss urban stations reliably represent the mixture of traffic and industrial emissions.

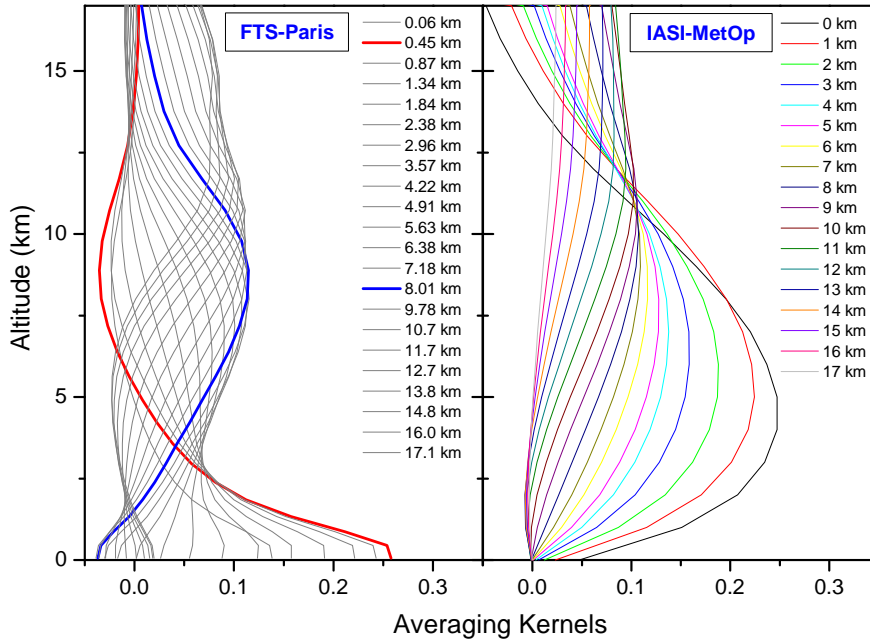


**Figure 5.** CO averaging kernels for each altitude of the a priori profile (from 0 to 17 km) for FTS-Paris (left panel) and IASI-MetOp (right panel).

In contrast, in situ surface CO at Jungfraujoch shows the same seasonal variability as the whole  
 425 atmosphere (characterized by the total column seasonality) and is shifted by 2 months with respect to  
 the urban sites. This is in agreement with the GEOS-Chem model at Jungfraujoch. Unlike the model  
 at Paris, where the underestimation is much stronger, GEOS-Chem underestimates the CO surface  
 VMR by about 23% at Jungfraujoch, which is similar to the 21% difference obtained for the total  
 columns. This is consistent with the much lower influence from low-altitude emissions and from the  
 430 PBL.

Figure 7 shows the monthly averaged surface CO in situ measurements performed at Wollon-  
 gong between June 2012 and May 2013. We observe a surface seasonality with a maximum around  
 October and a minimum in February-March. The maximum corresponds to elevated biomass burn-  
 ing levels during the Southern Hemisphere spring (Edwards et al., 2006). Unlike the two Northern  
 435 Hemisphere sites, there is no significant time shift between the CO seasonal variabilities at the Wol-  
 longong surface level and at higher altitudes. This suggests that the Wollongong surface atmosphere  
 is more representative of the free troposphere. The GEOS-Chem monthly averaged surface VMR  
 shows a maximum during the austral spring and a lower level after the end of the austral summer  
 until the austral winter. A striking increase after March 2013 is observed by the surface in situ mea-  
 440 surements, but not by the GEOS-Chem model. This might be due to nearby local emission sources



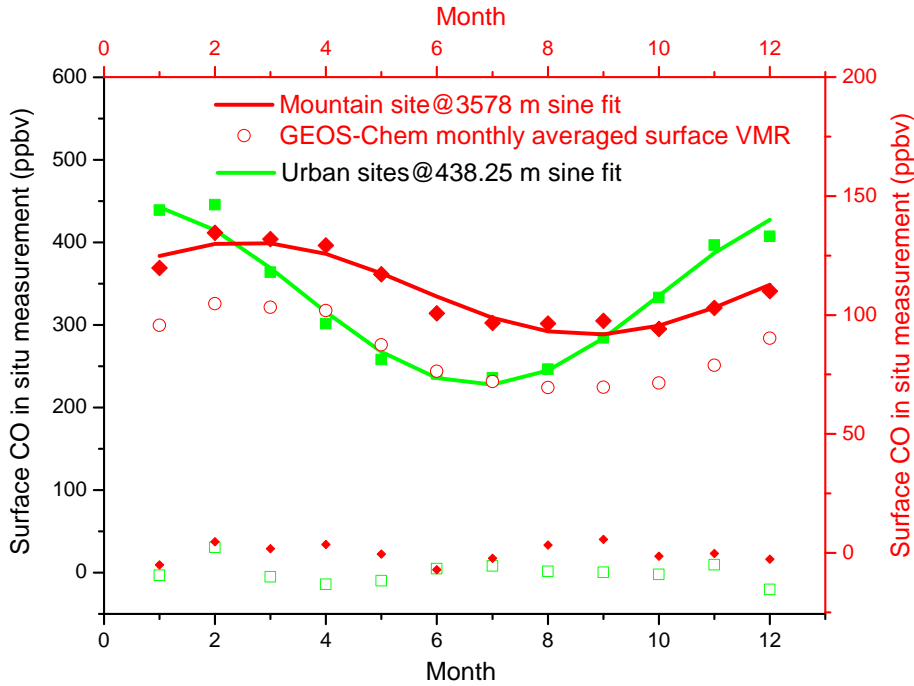


**Figure 6.** Monthly averaged CO in situ measurements at the surface in Switzerland using Swiss NABEL data from 2009 to 2013 (green squares are the means of the four urban sites and red diamonds are for Jungfrauoch). The sine function fit is applied to the 5 years monthly means of urban (green line) and mountain (red line) sites. The two lowermost datasets show the residuals of the fit (green open squares for urban sites and red small diamonds for Jungfrauoch). Monthly averaged CO surface VMR from GEOS-Chem located at Jungfrauoch is shown in red open circles.

which are probably not referenced in the inventories implemented in GEOS-Chem. A longer time series of these measurements will be helpful to better understand this observation. The background seasonality of CO is mainly driven by biomass burning sources modulated by the OH sink, (Buchholz et al., 2016). Similar to Paris, the surface CO discrepancy between model and measurement of  
 445  $-33\%$  is slightly increased as compared to the value of  $-20\%$  for the total columns.

### 4.3 Emission sources impacting the seasonality of CO columns

In order to study the influence of the different categories of CO and NMVOC emissions on the CO total column and its seasonality at the three sites, we perform three GEOS-Chem sensitivity simulations. These relied on the same setup as for the standard run (standard chemistry, horizontal  
 450 resolution, time period...), but in each of these simulations we turned off either the biogenic, the anthropogenic (incorporating the biofuel emissions) or the biomass burning emission sources implemented in the model. These categories include direct emissions of CO (for both anthropogenic

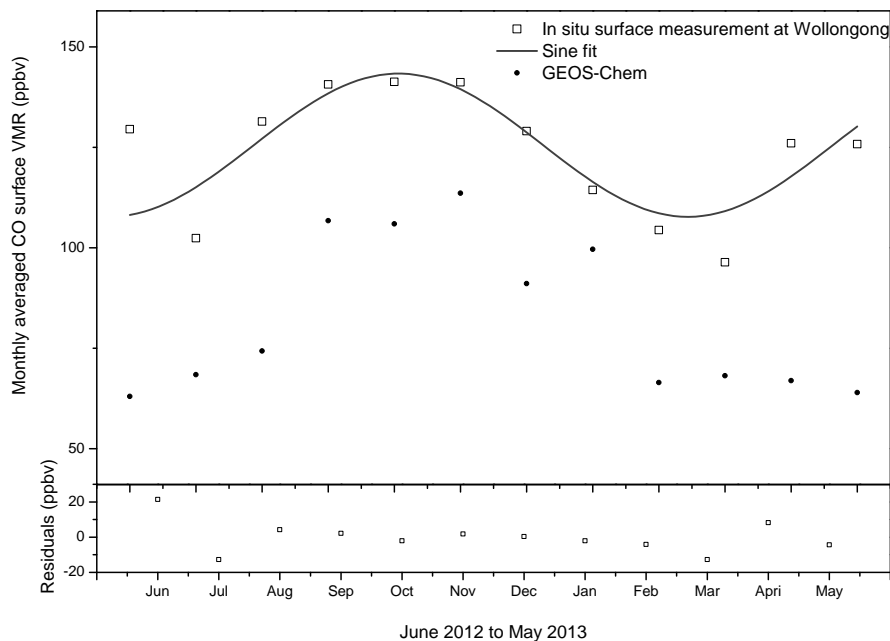


**Figure 7.** Monthly averaged CO surface VMR at Wollongong from in situ measurements (black open squares) and from GEOS-Chem model (black full circles) from June 2012 to May 2013. The sine function fit residuals are shown in the bottom panel.

and biomass burning sources) and its NMVOC precursor emissions, as well as direct emissions of nitric oxide (NO). In these three sensitivity runs – hereafter referred to as the non-biogenic, non-  
455 anthropogenic and non-biomass burning simulations –  $\text{CH}_4$  concentrations are based on measurements from NOAA. The results of these GEOS-Chem sensitivity simulations are compared to the standard run (results shown in Fig. 2). All four runs cover the mid-2005 to mid-2013 time period, hence starting a few years before our period under investigation. This allows us to establish a stable situation for the period 2008 (most of the long-lived precursors of CO are removed from the atmo-  
460 sphere between mid-2005 and 2008). Figure 8 shows the CO total columns simulated by the different runs of GEOS-Chem for the three sites. The results for Paris and Jungfraujoch are quite similar. At these two sites, the seasonal variability of the CO loadings is mainly driven by anthropogenic emissions. Indeed, by shutting off the anthropogenic emissions of CO and of its NMVOC precursors, the amplitude of the CO seasonal variation and periodicity are radically reduced. This is in agree-  
465 ment with previous model studies. Duncan et al. (2007) show that fossil fuel emissions are the main contribution to the CO burden in the Northern extra-tropics. The high-altitude Jungfraujoch site is strongly impacted by long-range transport of CO. At least one third of it is of non-European origin (Duncan et al., 2007; Zellweger et al., 2009). In comparison, shutting off either biomass burning or

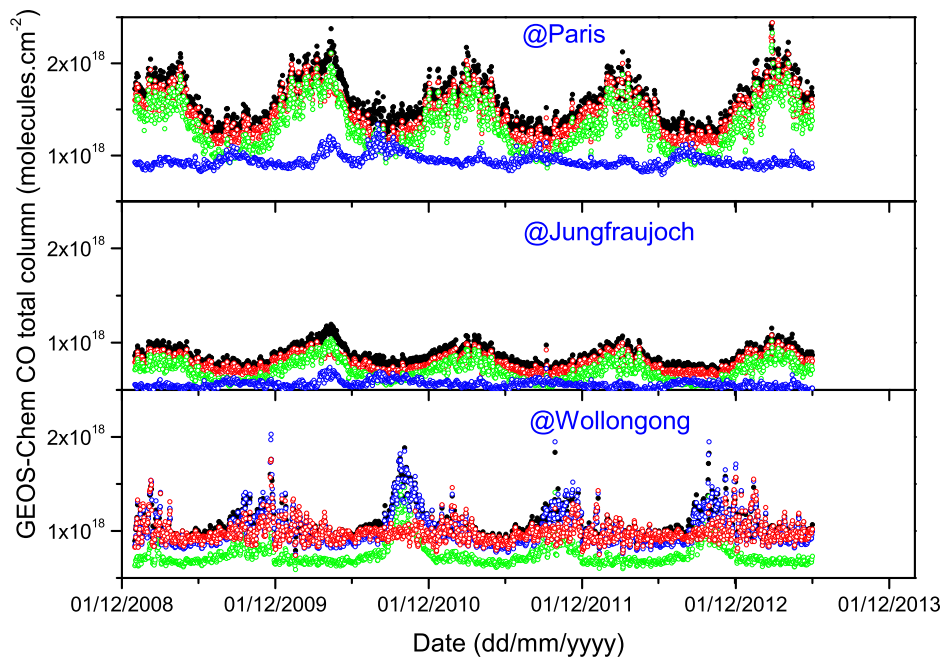


**Figure 8.** GEOS-Chem time series of CO total columns for Paris (top), Jungfraujoch (middle) and Wollongong (bottom). Different colors indicate standard run (black), run without biomass burning (red), run without biogenic emissions (green) and run without anthropogenic emissions (blue).

biogenic emissions, only weakly affects the seasonal variation and the maximum peaks. Compared  
 470 to the standard run, CO columns are marginally lower due to some missing emissions. At Wollon-  
 gong, the seasonal variability is mainly influenced by the biomass burning emissions: the highest  
 peaks (e.g. at the end of 2009) disappear when the biomass burning component is removed from the  
 simulation. The biogenic emissions provide the largest background contribution. Zeng et al. (2015)  
 have observed that the impact of biogenic emissions on CO is larger in the Southern Hemisphere  
 475 than in the Northern Hemisphere. Unlike at Paris and Jungfraujoch, the influence of anthropogenic  
 emissions is negligible in the Wollongong simulation. We also note that the GEOS-Chem sensitivity  
 runs provide the same results for the CO surface VMR, as for the CO total columns at the three  
 studied sites.

## 5 Conclusions

480 This paper investigates the seasonal variability of CO total columns at three NDACC and/or TCCON  
 sites: Paris and Jungfraujoch in the Northern Hemisphere and Wollongong in the Southern Hemi-  
 sphere. In the Northern Hemisphere, the variability of CO above the PBL has a seasonal maximum

in March-April and a minimum in September-October. In the Southern Hemisphere, this seasonal variation is shifted by 6 months. We have compared the ground-based FTIR data to satellite measurements from IASI-MetOp and MOPITT and to GEOS-Chem model standard outputs, which confirm the observed CO seasonal variability. However with currently implemented inventories, an underestimation of about 20% by the GEOS-Chem model is observed, which is consistent with previous forward and inverse modelling studies. Interestingly, a time-lag of about 2 months between upper altitude and surface CO has been found in the measurements and GEOS-Chem in both Paris and Jungfraujoch. This time lag is likely due to the different emission patterns. Custom simulations with emission sources being individually turned on and off show that the CO seasonality at Paris and Jungfraujoch is mainly controlled by anthropogenic emissions. In Wollongong, where low local anthropogenic emissions prevail and where the impact of biomass burning and biogenic emissions is large, such a time shift is neither observed nor modelled. We have thus observed a temporal shift in the seasonal patterns at the surface and in the higher atmospheric layers for the sites that are strongly affected by local anthropogenic emissions. The observation of the time-lag is likely due to zonal mixing occurring on a shorter (1–2 weeks) timescale than complete vertical tropospheric mixing (1–2 months). In the future, it will be interesting to study the link between local and non-local emission sources and the magnitude of the time shift between surface and total column CO by extending the present study to more sites and improving the analysis of the temporal signals. The presence of global ground-based FTIR networks provides a unique opportunity to obtain these data on a global scale, as the instruments are capable of sampling the surface and the total column data at the same time. The time lag data might also provide an additional benchmark parameter for chemical transport models and emission inventories, taking into account that the modeling of vertical CO gradients in the remote Southern Hemisphere already provides a challenge for chemical transport modeling (Fisher et al., 2015).

*Acknowledgements.* We are grateful to Université Pierre et Marie Curie and Région Île-de-France for their financial contributions and to Institut Pierre-Simon Laplace for support and facilities. We thank the National Center for Atmospheric Research MOPITT science team and NASA for producing and archiving the MOPITT CO product. Thanks are also due to the Swiss National Air Pollution Monitoring Network (NABEL) for delivering ground data around Switzerland. The University of Liège contribution to the present work has primarily been supported by the F.R.S. – FNRS, the Fédération Wallonie-Bruxelles and MeteoSwiss (GAW-CH program). We thank the International Foundation High Altitude Research Stations Jungfraujoch and Gornergrat (HFSJG, Bern). We are grateful to all colleagues who contributed to the acquisition of the FTIR data. The NDACC datasets used here are publicly available from the network database (<ftp://ftp.cpc.ncep.noaa.gov/ndacc/station>). The Australian Research Council has provided financial support over the years for the NDACC site at Wollongong, most recently as part of project DP110101948. We also acknowledge the important contribution to the measurement program at Wollongong made by researchers other than those listed as co-authors here, including amongst others, Voltaire Velazco and Nicholas Deutscher. IASI has been developed and built under the

520 responsibility of the French space agency CNES. It is flown onboard the MetOp satellite as part of the Eumet-  
sat Polar System (EPS). The IASI L1 data are received through the Eumetcast near real time data distribution  
service. IASI L1 and L2 data are stored in the French atmospheric database Ether (<http://ether.ipsl.jussieu.fr>).  
The National Center for Atmospheric Research (NCAR) is sponsored by the National Science Foundation. Any  
opinions, findings and conclusions or recommendations expressed in the publication are those of the author(s)  
525 and do not necessarily reflect the views of the National Science Foundation.

[Table 1 about here.]

[Table 2 about here.]

## References

- August, T., Klaes, D., Schlüssel, P., Hultberg, T., Crapeau, M., Arriaga, A., O'Carroll, A., Coppens, D., Munro,  
530 R., and Calbet, X.: IASI on MetOp-A: Operational Level 2 retrievals after five years in orbit, *J. Quant.  
Spectroscop. Radiat. Transfer*, 113, 1340–1371, doi:10.1016/j.jqsrt.2012.02.028, 2012.
- Bakwin, P. S., Tans, P. P., and Novelli, P. C.: Carbon monoxide budget in the northern hemisphere, *Geophys.  
Res. Lett.*, 21, 433–436, 1994.
- Barret, B., Mazière, D. M., and Mahieu, E.: Ground-based FTIR measurements of CO from the Jungfrauoch:  
535 characterisation and comparison with in situ surface and MOPITT data, *Atmos. Chem. Phys.*, 3, 2217–2223,  
doi:10.5194/acp-3-2217-2003, 2003.
- Bekki, S., Law, K. S., and Pyle, J. A.: Effect of ozone depletion on atmospheric CH<sub>4</sub> and CO concentrations,  
*Nature*, 371, 595–597, doi:10.1038/371595a0, 1994.
- Benedictow, A., Berge, H., Fagerli, H., Gauss, M., Jonson, J. E., Nyíri, A., Simpson, D., Tsyro, S., Valdebenito,  
540 A., Shamsudheen, V. S., Wind, P., Aas, W., Hjellbrekke, A.-G., Mareckova, K., Wankmüller, R., Iversen,  
T., Kirkevåg, A., Seland, Ø., Haugen, J. E., and Mills, G.: Transboundary acidification, eutrophication and  
ground level ozone in Europe in 2008, Tech. rep., The Norwegian Meteorological Institute, Oslo, Norway,  
2010.
- Bey, I., Jacob, D. J., Yantosca, R. M., Logan, J. A., Field, B. D., Fiore, A. M., Li, Q., Liu, H. Y., Mickley, L. J.,  
545 and Schultz, M. G.: Global modeling of tropospheric chemistry with assimilated meteorology: model de-  
scription and evaluation, *J. Geophys. Res.-Atmos.*, 106, 23 073–23 095, doi:10.1029/2001JD000807, 2001.
- Blumstein, D., Chalon, G., Carlier, T., Buil, C., Hebert, P., Maciaszek, T., Ponce, G., Phulpin, T., Tournier, B.,  
Simeoni, D., Astruc, P., Clauss, A., Kayal, G., and Jegou, R.: IASI instrument: technical overview and mea-  
sured performances, in: *Proc. SPIE 5543, Infrared Spaceborne Remote Sensing XII*, doi:10.1117/12.560907,  
550 2004.
- Bousquet, P., Hauglustaine, D. A., Peylin, P., Carouge, C., and Ciais, P.: Two decades of OH variability as  
inferred by an inversion of atmospheric transport and chemistry of methyl chloroform, *Atmos. Chem. Phys.*,  
5, 2635–2656, doi:10.5194/acp-5-2635-2005, 2005.
- Brunke, E.-G., Scheel, H., and Seiler, W.: Trends of tropospheric CO, N<sub>2</sub>O and CH<sub>4</sub> as observed at cape point,  
555 South Africa, *Atmos. Environ.*, 24, 585–595, doi:10.1016/0960-1686(90)90013-D, 1990.
- Buchholz, R. R., Paton-Walsh, C., Griffith, D. W. T., Kubistin, D., Caldow, C., Fisher, J. A., Deutscher, N. M.,  
Kettlewell, G., Riggensbach, M., Macatangay, R., Krummel, P. B., and Langenfelds, R. L.: Source and meteo-  
rological influences on air quality (CO, CH<sub>4</sub> & CO<sub>2</sub>) at a Southern Hemisphere urban site, *Atmos. Environ.*,  
126, 274–289, doi:10.1016/j.atmosenv.2015.11.041, 2016.
- 560 Clerbaux, C., George, M., Turquety, S., Walker, K. A., Barret, B., Bernath, P., Boone, C., Borsdorff, T., Cammas,  
J. P., Catoire, V., Coffey, M., Coheur, P.-F., Deeter, M., Mazière, D. M., Drummond, J., Duchatelet, P., Dupuy,  
E., Zafra, d. R., Eddounia, F., Edwards, D. P., Emmons, L., Funke, B., Gille, J., Griffith, D. W. T., Hannigan,  
J., Hase, F., Höpfner, M., Jones, N., Kagawa, A., Kasai, Y., Kramer, I., Flochmoën, L. E., Livesey, N. J.,  
López-Puertas, M., Luo, M., Mahieu, E., Murtagh, D., Nédélec, P., Pazmino, A., Pumphrey, H., Ricaud, P.,  
565 Rinsland, C. P., Robert, C., Schneider, M., Senten, C., Stiller, G., Strandberg, A., Strong, K., Sussmann,  
R., Thouret, V., Urban, J., and Wiacek, A.: CO measurements from the ACE-FTS satellite instrument: data

- analysis and validation using ground-based, airborne and spaceborne observations, *Atmos. Chem. Phys.*, 8, 2569–2594, doi:10.5194/acp-8-2569-2008, 2008.
- 570 Clerbaux, C., Boynard, A., Clarisse, L., George, M., Hadji-Lazarou, J., Herbin, H., Hurtmans, D., Pommier, M., Razavi, A., Turquety, S., Wespes, C., and Coheur, P.-F.: Monitoring of atmospheric composition using the thermal infrared IASI/MetOp sounder, *Atmos. Chem. Phys.*, 9, 6041–6054, doi:10.5194/acp-9-6041-2009, 2009.
- 575 Deeter, M., Emmons, L., Francis, G., Edwards, D., Gille, J., Warner, J., Khattatov, B., Ziskin, D., Lamarque, J.-F., Ho, S.-P., Yudin, V., Attié, J.-L., Packman, D., Chen, J., Mao, D., Drummond, J., Novelli, P., and Sachse, G.: Evaluation of operational radiances for the Measurements of Pollution in the Troposphere (MOPITT) instrument CO thermal band channels, *J. Geophys. Res.*, 109, D03 308, doi:10.1029/2003JD003970, 2004.
- Dils, B., Cui, J., Henne, S., Mahieu, E., Steinbacher, M., and Mazière, D. M.: CO trend at the high Alpine site Jungfraujoch: a comparison between NDIR surface in situ and FTIR remote sensing observations, *Atmos. Chem. Phys.*, 11, 6735–6748, doi:10.5194/acp-11-6735-2011, 2011.
- 580 Drummond, J. and Mand, G.: The Measurements of Pollution in the Troposphere (MOPITT) Instrument: Overall Performance and Calibration Requirements, *J. Atmos. Ocean. Technol.*, 13, 314, 1996.
- Duchatelet, P., Demoulin, P., Hase, F., Ruhnke, R., Feng, W., Chipperfield, M. P., Bernath, P. F., Boone, C. D., Walker, K. A., and Mahieu, E.: Hydrogen fluoride (HF) total and partial column time series above the Jungfraujoch from long-term FTIR measurements: impact of the line-shape model, error budget, seasonal cycle and comparison with satellite and model data, *J. Geophys. Res.*, 115, D22 306, doi:10.1029/2010JD014677, 2010.
- 585 Duncan, B. N., Logan, J. A., Bey, I., Megretskaia, I. A., Yantosca, R. M., Novelli, P. C. Jones, N. B., and Rinsland, C. P.: Global budget of CO, 1988–1997: Source estimates and validation with a global model, *J. Geophys. Res. Atmos.*, 112, doi:10.1029/2007JD008459, d22301, 2007.
- 590 Edwards, D. P., Pétron, G., Novelli, P. C., Emmons, L. K., Gille, J. C., and Drummond, J. R.: Southern Hemisphere carbon monoxide interannual variability observed by Terra/Measurement of Pollution in the Troposphere (MOPITT), *J. Geophys. Res.*, 111, D16 303, doi:10.1029/2006JD007079, 2006.
- Esposito, F., Grieco, G., Masiello, G., Pavese, G., Restieri, R., Serio, C., and Cuomo, V.: Intercomparison of line-parameter spectroscopic databases using downwelling spectral radiance, *Quart. J. Roy. Met. Soc.*, 133, 191–202, doi:10.1002/qj.131, 2007.
- 595 Fisher, J. A., Wilson, S. R., Zeng, G., Williams, J. E., Emmons, L. K., Langenfelds, R. L., Krummel, P. B., and Steele, L. P.: Seasonal changes in the tropospheric carbon monoxide profile over the remote Southern Hemisphere evaluated using multi-model simulations and aircraft observations, *Atmos. Chem. Phys.*, 15, 3217–3239, doi:10.5194/acp-15-3217-2015, 2015.
- 600 George, M., Clerbaux, C., Hurtmans, D., Turquety, S., Coheur, P.-F., Pommier, M., Hadji-Lazarou, J., Edwards, D. P., Worden, H., Luo, M., Rinsland, C., and McMillan, W.: Carbon monoxide distributions from the IASI/METOP mission: evaluation with other space-borne remote sensors, *Atmos. Chem. Phys.*, 9, 8317–8330, doi:10.5194/acp-9-8317-2009, 2009.
- Griffith, D. W. T.: Synthetic Calibration and Quantitative Analysis of Gas-Phase infrared Spectra, *Appl. Spectroscop.*, 50, 59–70, 1996.
- 605

- Griffith, D. W. T., Deutscher, N. M., Caldow, C. G. R., Kettlewell, G., Riggenbach, M., and Hammer, S.: A Fourier transform infrared trace gas and isotope analyser for atmospheric applications, *Atmos. Meas. Tech.*, 5, 2012.
- 610 Guenther, A., Karl, T., Harley, P., Wiedinmyer, C., Palmer, P. I., and Geron, C.: Estimates of global terrestrial isoprene emissions using MEGAN (Model of Emissions of Gases and Aerosols from Nature), *Atmos. Chem. Phys.*, 6, 10–5194, 2006.
- Hase, F., Hannigan, J. W., Coey, M. T., Goldman, A., Höpfner, M., Jones, N. B., Rinsland, C. P., and Wood, S. W.: Intercomparison of retrieval codes used for the analysis of high-resolution: ground-based FTIR measurements, *J. Quant. Spectroscop. Radiat. Transfer*, 87, 25–52, 2004.
- 615 Hase, F., Demoulin, P., Sauval, A. J., Toon, G. C., Bernath, P. F., Goldman, A., Hannigan, J. W., and Rinsland, C. P.: An empirical line-by-line model for the infrared solar transmittance spectrum from 700 to 5000  $\text{cm}^{-1}$ , *J. Quant. Spectroscop. Radiat. Transfer*, 102, 450–463, doi:10.1016/j.jqsrt.2006.02.026, 2006.
- Holloway, T., Levy, H., and Kasibhatla, P.: Global distribution of carbon monoxide, *J. Geophys. Res. Atmos.*, 105, 12 123–12 147, doi:10.1029/1999JD901173, 2000.
- 620 Hooghiemstra, P. B., Krol, M. C., Bergamaschi, P., de Laat, A. T. J., van der Werf, G. R., Novelli, P. C., Deeter, M. N., Aben, I., and Röckmann, T.: Comparing optimized CO emission estimates using MOPITT or NOAA surface network observations, *J. Geophys. Res.*, 117, D06 309–23, 2012.
- Hurtmans, D., Coheur, P.-F., Wespes, C., Clarisse, L., Scharf, O., Clerbaux, C., Hadji-Lazaro, J., George, M., and Turquety, S.: FORLI radiative transfer and retrieval code for IASI, *J. Quant. Spectroscop. Radiat. Transfer*, 113, 1391–1408, doi:10.1016/j.jqsrt.2012.02.036, 2006.
- 625 Khalil, M. A. K. and Rasmussen, R. A.: Carbon monoxide in the Earth’s atmosphere: indications of a global increase, *Nature*, 332, 242–245, doi:10.1038/332242a0, 1988.
- Khalil, M. A. K. and Rasmussen, R. A.: Global decrease in atmospheric carbon monoxide concentration, *Nature*, 370, 639–641, doi:10.1038/370639a0, 1994.
- 630 Kopacz, M., Jacob, D. J., Fisher, J. A., Logan, J. A., Zhang, L., Megretskaya, I. A., Yantosca, R. M., Singh, K., Henze, D. K., Burrows, J. P., Buchwitz, M., Khlystova, I., McMillan, W. W., Gille, J. C., Edwards, D. P., Eldering, A., Thouret, V., and Nedelec, P.: Global estimates of CO sources with high resolution by adjoint inversion of multiple satellite datasets (MOPITT, AIRS, SCIAMACHY, TES), *Atmos. Chem. Phys.*, 10, 855–876, 2010.
- 635 Logan, J. A., Prather, M. J., Wofsy, F. C., and McElroy, M. B.: Tropospheric Chemistry: A Global Perspective, *J. Geophys. Res.*, 86, 7210–7254, 1981.
- Mahieu, E., Zander, R., Delbouille, L., Demoulin, P., Roland, G., and Servais, C.: Observed Trends in Total Vertical Column Abundances of Atmospheric Gases from IR Solar Spectra Recorded at the Jungfraujoch, *J. Atmos. Chem.*, 28, 227–243, doi:10.1023/A:1005854926740, 1997.
- 640 Mao, J., Jacob, D. J., Evans, M. J., Olson, J. R., Ren, X., Brune, W. H., Clair, S. J. M., Crounse, J. D., Spencer, K. M., Beaver, M. R., Wennberg, P. O., Cubison, M. J., Jimenez, J. L., Fried, A., Weibring, P., Walega, J. G., Hall, S. R., Weinheimer, A. J., Cohen, R. C., Chen, G., Crawford, J. H., McNaughton, C., Clarke, A. D., Jaeglé, L., Fisher, J. A., Yantosca, R. M., Sager, L. P., and Carouge, C.: Chemistry of hydrogen oxide radicals (HOx) in the Arctic troposphere in spring, *Atmos. Chem. Phys.*, 10, 5823–5838, doi:10.5194/acp-10-5823-2010, 2010.
- 645



- Novelli, P. C., Masarie, K. A., Tans, P. P., and Lang, P. M.: Recent Changes in Atmospheric Carbon Monoxide, *Science*, 263, 1587–1590, doi:10.1126/science.263.5153.1587, 1994.
- Novelli, P. C., Masarie, K. A., and Lang, P. M.: Distributions and recent changes of carbon monoxide in the lower troposphere, *J. Geophys. Res. Atmos.*, 103, 19 015–19 033, doi:10.1029/98JD01366, 1998.
- 650 Novelli, P. C., Masarie, K. A., Lang, P. M., Hall, B. D., Myers, R. C., and Elkins, J. W.: Reanalysis of tropospheric CO trends: Effects of the 1997–1998 wildfires, *J. Geophys. Res. Atmos.*, 108, doi:10.1029/2002JD003031, 4464, 2003.
- Olivier, J. G. J. and Berdowski, J. J. M.: Global emissions sources and sinks., in: *The Climate System*, edited by Berdowski, J., Guicherit, R., and Heij, B., pp. 33–78, A.A. Balkema Publishers/Swets & Zeitlinger Publishers, Lisse, The Netherlands, 2001.
- 655 Park, R. J., Jacob, D. J., Field, B. D., Yantosca, R. M., and Chin, M.: Natural and transboundary pollution influences on sulfate-nitrate-ammonium aerosols in the United States: implications for policy, *J. Geophys. Res.*, 109, D15 204, doi:10.1029/2003JD004473, 2004.
- Pougatchev, N. S. and Rinsland, C. P.: Spectroscopic study of the seasonal variation of carbon monoxide vertical distribution above Kitt Peak, *J. Geophys. Res.*, 100, 1409–1416, 1995.
- 660 Rinsland, C. P., Jones, N. B., Connor, B. J., Logan, J. A., Pougatchev, N. S., Goldman, A., Murcray, F. J., Stephen, T. M., Pine, A. S., Zander, R., Mahieu, E., and Demoulin, P.: Northern and southern hemisphere ground-based infrared spectroscopic measurements of tropospheric carbon monoxide and ethane, *J. Geophys. Res.*, 103, 28 197, doi:10.1029/98JD02515, 1998.
- 665 Rinsland, C. P., Goldman, A., Murcray, F. J., Stephen, T. M., Pougatchev, N. S., Fishman, J., David, S. J., Blatherwick, R. D., Novelli, P. C., Jones, N. B., and Connor, B. J.: Infrared solar spectroscopic measurements of free tropospheric CO, C<sub>2</sub>H<sub>6</sub>, and HCN above Mauna Loa, Hawaii: Seasonal variations and evidence for enhanced emissions from the Southeast Asian tropical fires of 1997–1998, *J. Geophys. Res. Atmos.*, 104, 18 667–18 680, doi:10.1029/1999JD900366, 1999.
- 670 Rinsland, C. P., Mahieu, E., Zander, R., Demoulin, P., Forrer, J., and Buchmann, B.: Free tropospheric CO, C<sub>2</sub>H<sub>6</sub>, and HCN above central Europe: Recent measurements from the Jungfraujoch station including the detection of elevated columns during 1998, *J. Geophys. Res.*, 105, 24 235–24 249, 2000.
- Rinsland, C. P., Meier, A., Griffith, D. W. T., and Chiou, L. S.: Ground-based measurements of tropospheric CO, C<sub>2</sub>H<sub>6</sub>, and HCN from Australia at 34°S latitude during 1997–1998, *J. Geophys. Res. Atmos.*, 106,
- 675 20 913–20 924, doi:10.1029/2000JD000318, 2001.
- Rinsland, C. P., Goldman, A., Hannigan, J. W., Wood, S. W., Chiou, L. S., and Mahieu, E.: Long-term trends of tropospheric carbon monoxide and hydrogen cyanide from analysis of high resolution infrared solar spectra, *J. Quant. Spectroscop. Radiat. Transfer*, 104, 40–51, 2007.
- Rodgers, C. D.: Characterization and error analysis of profiles retrieved from remote sounding measurements, *J. Geophys. Res.*, 95, doi:10.1029/JD095iD05p05587, 1990.
- 680 Rodgers, C. D. and Connor, B. J.: Intercomparison of remote sounding instruments, *J. Geophys. Res.*, 108, 4116–4129, doi:10.1029/2002JD002299, 2003.
- Rohrer, F. and Berresheim, H.: Strong correlation between levels of tropospheric hydroxyl radicals and solar ultraviolet radiation, *Nature*, 442, 184–187, doi:10.1038/nature04924, 2006.

- 685 Rothman, L. S., Jacquemart, D., Barbe, A., Benner, D. C., Birk, M., Brown, L. R., Carleer, M. R., Chackerian, Jr. C., Chance, K., Coudert, L. H., Dana, V., Devi, V. M., Flaud, J.-M., Gamache, R. R., Goldman, A., Hartmann, J.-M., Jucks, K. W., Maki, A. G., Mandin, J.-Y., Massie, S. T., Orphal, J., Perrin, A., Rinsland, C. P., Smith, M. A. H., Tennyson, J., Tolchenov, R. N., Toth, R. A., Vander Auwera, J., Varanasi, P., and Wagner, G.: The HITRAN 2004 Molecular Spectroscopic Database, *J. Quant. Spectrosc. Radiat. Trans.*, 96, 139 – 204, 2005.
- 690 Rothman, L. S., Gordon, I. E., Barbe, A., Benner, D. C., Bernath, P. F., Birk, M., Boudon, V., Brown, L. R., Campargue, A., Champion, J. P., Chance, K., Coudert, L. H., Dana, V., Devi, V. M., Fally, S., Flaud, J. M., Gamache, R. R., Goldman, A., Jacquemart, D., Kleiner, I., Lacombe, N., Lafferty, W. J., Mandin, J. Y., Massie, S. T., Mikhailenko, S. N., Miller, C. E., Moazzen-Ahmadi, N., Naumenko, O. V., Nikitin, A. V., Orphal, J., Perevalov, V. I., Perrin, A., Predoi-Cross, A., Rinsland, C. P., Rotger, M., Simecková, M., Smith, M. A. H., Sung, K., Tashkun, S. A., Tennyson, J., Toth, R. A., Vandaele, A. C., and Vander Auwera, J.: The HITRAN 2008 molecular spectroscopic database, *J. Quant. Spectrosc. Radiat. Trans.*, 110, 533–572, 2009.
- Schneider, M., Yoshimura, K., Hase, F., and Blumenstock, T.: The ground-based FTIR network's potential for investigating the atmospheric water cycle, *Atmos. Chem. Phys.*, 10, 3427–3442, 2010.
- 700 Schultz, M., Backman, L., Balkanski, Y., Bjoernsdalsaeter, S., Brand, R., Burrows, J., Dalsoeren, S., de Vasconcelos, M., Grodtmann, B., Hauglustaine, D., Heil, A., Hoelzemann, J., Isaksen, I., Kaurola, J., Knorr, W., Ladstaetter-Weissenmayer, A., Mota, B., Oom, D., Pacyna, J., Panasiuk, D., Pereira, J., Pulles, T., Pyle, J., Rast, S., Richter, A., Savage, N., Schnadt, C., Schulz, M., Spessa, A., Staehelin, J., Sundet, J., Szopa, S., Thonicke, K., van het Bolscher, M., van Noije, T., van Velthoven, P., Vik, A., and Wittrock, F.: REanalysis of the TROpospheric chemical composition over the past 40 years – A long-term global modeling study of tropospheric chemistry, final report 48/2007, Max Planck Institute for Meteorology, Hamburg, Germany, 2007.
- 705 Street, J. O., Carroll, R. J., and Ruppert, D.: A Note on Computing Robust Regression Estimates via Iteratively Reweighted Least Squares, *Am. Stat.*, 42, 152–154, doi:10.1080/00031305.1988.10475548, 1988.
- 710 Té, Y., Jeseck, P., Payan, S., Pépin, I., and Camy-Peyret, C.: The Fourier transform spectrometer of the UPMC University QualAir platform, *Rev. Sci. Instrum.*, 81, 103 102–10, doi:10.1063/1.3488357, 2010.
- Té, Y., Dieudonné, E., Jeseck, P., Hase, F., Hadji-Lazaro, J., Clerbaux, C., Ravetta, F., Payan, S., Pépin, I., Hurtmans, D., Pelon, J., and Camy-Peyret, C.: Carbon monoxide urban emission monitoring: a ground-based FTIR case study, *J. Atmos. Oceanic Technol.*, 29, 911–921, doi:10.1175/JTECH-D-11-00040.1, 2012.
- 715 Thompson, A. M.: The oxidizing capacity of the earth's atmosphere: Probable past and future changes, *Science*, 286, 1157–1165, doi:10.1126/science.256.5060.1157, 1992.
- Thompson, A. M., Huntley, M. A., and Stewart, R. W.: Perturbations to tropospheric oxidants, 1985–2035: 1. Calculations of ozone and OH in chemically coherent regions, *J. Geophys. Res.*, 95, 9829–9844, doi:10.1029/JD095iD07p09829, 1990.
- 720 Tournier, B., Blumstein, D., Cayla, F.-R., and Chalon, G.: IASI level 0 and 1 processing algorithms description, in: *Proc. 12<sup>th</sup> Int. TOVS Study Conf. (ITSC-XII)*, Lorne, VIC, Australia, 2002.
- van der Werf, G. R., Randerson, J. T., Giglio, L., Collatz, G. J., Mu, M., Kasibhatla, P. S., Morton, D. C., DeFries, R. S., Jin, Y., and Leeuwen, v. T. T.: Global fire emissions and the contribution of deforestation,

- savanna, forest, agricultural, and peat fires, *Atmos. Chem. Phys.*, 10, 11 707–11 735, doi:10.5194/acp-10-11707-2010, 2010.
- 725 van Donkelaar, A., Martin, R. V., Leaitch, W. R., MacDonald, A. M., Walker, T. W., Streets, D. G., Zhang, Q., Dunlea, E. J., Jimenez, J. L., Dibb, J. E., Huey, L. G., Weber, R., and Andreae, M. O.: Analysis of aircraft and satellite measurements from the Intercontinental Chemical Transport Experiment (INTEX-B) to quantify long-range transport of East Asian sulfur to Canada, *Atmos. Chem. Phys.*, 8, 10–5194, doi:10.5194/acp-8-2999-2008, 2008.
- 730 Viatte, C., Schneider, M., Redondas, A., Hase, F., Eremenko, M., Chelin, P., Flaud, J.-M., Blumenstock, T., and Orphal, J.: Comparison of ground-based FTIR and Brewer O<sub>3</sub> total column with data from two different IASI algorithms and from OMI and GOME-2 satellite instruments, *Atmos. Meas. Tech.*, 4, 535–546, doi:10.5194/amt-4-535-2011, 2011.
- 735 Weinstock, B.: Carbon Monoxide: Residence Time in the Atmosphere, *Science*, 166, 224–225, 1969.
- Worden, H. M., Deeter, M. N., Edwards, D. P., Gille, J. C., Drummond, J. R., and Nédélec, P.: Observations of near-surface carbon monoxide from space using MOPITT multispectral retrievals, *J. Geophys. Res. Atmos.*, 115, doi:10.1029/2010JD014242, d18314, 2010.
- Xiao, Y., Logan, J. A., Jacob, D. J., Hudman, R. C., Yantosca, R., and Blake, D. R.: Global budget of ethane and regional constraints on U.S. sources, *J. Geophys. Res.*, 113, 21 306–10, doi:10.1029/2007JD009415, 2008.
- 740 Yurganov, L. N., Blumenstock, T., Grechko, E. I., Hase, F., Hyer, E. J., Kasischke, E. S., Koike, M., Kondo, Y., Kramer, I., Leung, F.-Y., Mahieu, E., Mellqvist, J., Notholt, J., Novelli, P. C., Rinsland, C. P., Scheel, H. E., Schulz, A., Strandberg, A., Sussmann, R., Tanimoto, H., Velazco, V., Zander, R., and Zhao, Y.: A quantitative assessment of the 1998 carbon monoxide emission anomaly in the Northern Hemisphere based on total column and surface concentration measurements, *J. Geophys. Res. Atmos.*, 109, doi:10.1029/2004JD004559, d15305, 2004.
- 745 Yurganov, L. N., Duchatelet, P., Dzhola, A. V., Edwards, D. P., Hase, F., Kramer, I., Mahieu, E., Mellqvist, J., Notholt, J., Novelli, P. C., Rockmann, A., Scheel, H. E., Schneider, M., Schulz, A., Strandberg, A., Sussmann, R., Tanimoto, H., Velazco, V., Drummond, J. R., and Gille, J. C.: Increased Northern Hemispheric carbon monoxide burden in the troposphere in 2002 and 2003 detected from the ground and from space, *Atmos. Chem. and Phys.*, 5, 563–573, doi:10.5194/acp-5-563-2005, 2005.
- 750 Zander, R., Demoulin, P., Ehhalt, D. H., Schmidt, U., and Rinsland, C. P.: Secular increase of the total vertical column abundance of carbon monoxide above central Europe since 1950, *J. Geophys. Res. Atmos.*, 94, 11 021–11 028, doi:10.1029/JD094iD08p11021, 1989.
- 755 Zander, R., Mahieu, E., Demoulin, P., Duchatelet, P., Roland, G., Servais, C., Mazière, D. M., Reimann, S., and Rinsland, C. P.: Our changing atmosphere: Evidence based on long-term infrared solar observations at the Jungfraujoch since 1950, *Sci. Tot. Environ.*, 391, 184–195, doi:10.1016/j.scitotenv.2007.10.018, 2008.
- Zbinden, R. M., Thouret, V., Ricaud, P., Carminati, F., Cammas, J.-P., and Nédélec, P.: Climatology of pure tropospheric profiles and column contents of ozone and carbon monoxide using MOZAIC, *Atmos. Chem. Phys.*, 13, 12 363–12 388, doi:10.5194/acp-13-12363-2013, 2013.
- 760 Zellweger, C., Hüglin, C., Klausen, J., Steinbacher, M., Vollmer, M., and Buchmann, B.: Inter-comparison of four different carbon monoxide measurement techniques and evaluation of the long-term carbon monoxide time series of Jungfraujoch, *Atmos. Chem. Phys.*, 9, 3491–3503, doi:10.5194/acp-9-3491-2009, 2009.

- Zeng, G., Williams, J. E., Fisher, J. A., Emmons, L. K., Jones, N. B., Morgenstern, O., Robinson, J., Smale, D., Paton-Walsh, C., and Griffith, D. W. T.: Multi-model simulation of CO and HCHO in the Southern Hemisphere: comparison with observations and impact of biogenic emissions, *Atmos. Chem. Phys.*, 15, 7217–7245, 2015.
- Zhao, Y., Kondo, Y., Murcray, F. J., Liu, X., Koike, M., Kita, K., Nakajima, H., Murata, I., and Suzuki, K.: Carbon monoxide column abundances and tropospheric concentrations retrieved from high resolution ground-based infrared solar spectra at 43.5°N over Japan, *J. Geophys. Res.*, 102, 23 403–23 411, 1997.
- Zhao, Y., Strong, K., Kondo, Y., Koike, M., Matsumi, Y., Irie, Y., Rinsland, H., C, P., Jones, N. B., Suzuki, K., Nakajima, H., Nakane, H., and Murata, I.: Spectroscopic measurements of tropospheric CO, C<sub>2</sub>H<sub>6</sub>, C<sub>2</sub>H<sub>2</sub> and HCN in Northern Japan, *J. Geophys. Res.*, 107, 4343, doi:10.1029/2001JD000748, 2002.

**Table 1.** Ground-based FTIR instrument parameters for the three measurement stations

	Paris	Jungfraujoch	Wollongong
Sun-tracker model	A547 (Bruker Optics)	Home made	A547 (Bruker Optics)
Sun-tracker accuracy	< 1 arcmin	< 6 arcmin	< 1 arcmin
Spectrometer	IFS 125HR	IFS 120HR	IFS 125HR
Network	TCCON with NDACC measurements	NDACC	NDACC and TCCON
Optical Path Difference	257 cm	114 to 175 cm	257 cm
Integration time	205 s	135 to 1035 s	206 s
	(2 co-additions)	(depending on co-addition and OPD)	(2 co-additions)
Entrance window	CaF <sub>2</sub> (instrument under vacuum)	None (instrument not under vacuum)	KBr (instrument under vacuum)
Beamsplitter	CaF <sub>2</sub>	KBr	CaF <sub>2</sub>
Optical filter	Yes	Yes	Yes
Detector	InSb	InSb	InSb
Spectral range	3.8 to 5.1 $\mu\text{m}$	4.4 to 6 $\mu\text{m}$	4.4 to 5.1 $\mu\text{m}$

**Table 2.** Parameters obtained from the sinusoidal fit of the seasonal variability to the CO total columns from ground-based, satellite and GEOS-Chem modeling data

	Paris		Jungfrauoch		Wollongong	
	Half-period ( $w$ ) (days)	Amplitude ( $A$ ) (%)	Half-period ( $w$ ) (days)	Amplitude ( $A$ ) (%)	Half-period ( $w$ ) (days)	Amplitude ( $A$ ) (%)
Ground-based	$191 \pm 3$	$14 \pm 1$	$185 \pm 1$	$12 \pm 1$	$178 \pm 1$	$17 \pm 1$
Satellite data	$183 \pm 1$	$14 \pm 1$	$190 \pm 2$	$12 \pm 1$	$182 \pm 1$	$16 \pm 1$
GEOS-Chem	$183 \pm 1$	$19 \pm 1$	$182 \pm 1$	$12 \pm 1$	$180 \pm 1$	$13 \pm 1$